Temperature effects on phase equilibrium and diffusion in mesopores

Muslim Dvoyashkin, Rustem Valiullin,* and Jörg Kärger
Fakultät für Physik und Geowissenschaften, Universität Leipzig, 04103 Leipzig, Germany
(Received 8 January 2007; revised manuscript received 21 February 2007; published 27 April 2007)

The equilibrium and dynamic properties of fluids confined to mesoporous material have been studied using nuclear magnetic resonance (NMR) methods. Molecular diffusion of *n*-pentane in Vycor porous glass within closed sample tubes has been measured by means of the pulsed field gradient (PFG) NMR method for temperatures notably exceeding the boiling point of the neat liquid. It is found that the temperature dependence of the diffusivity dramatically depends on the state of the fluid surrounding the mesoporous monoliths. In an oversaturated sample, i.e., in a sample containing some amount of the liquid also outside of the porous material, the diffusivity in the mesopores followed the Arrhenius dependence. In samples with only the mesopores saturated by the liquid, i.e., without any excess fluid, with increasing temperature the diffusivity notably deviated from the Arrhenius dependence towards higher diffusivities. The analysis of the intensities of the respective NMR signals from the fluid within the porous material and in the surrounding phase has revealed that this anomaly is accompanied by the formation of a space free of liquid within the pore system. With the measured pore filling factors, the resulting overall diffusivity is estimated by a two-region approach with diffusion occurring in either the liquid phase or the free space within the pore volume. It is shown that this procedure, free of any fitting parameters, yields excellent agreement with the experimental data.

DOI: 10.1103/PhysRevE.75.041202 PACS number(s): 51.20.+d, 61.43.Gt, 64.70.Fx

I. INTRODUCTION

Molecules confined within pores of mesoscopic scale can exhibit a series of properties differing from that of the bulk liquid. The interactions with pore walls and competition between fluid-wall and fluid-fluid interactions may lead to various surface-driven effects [1–4]. One of the important characteristics which reflect the dynamical properties of fluids is the coefficient of self-diffusion. Because diffusion is very sensitive to local interactions, both energetic and steric ones, it may yield information on the properties of a confining medium on length scales of the order of the pore sizes. This has been, in particular, demonstrated in many studies using the pulsed field gradient (PFG) nuclear magnetic resonance (NMR) method. It turned out to be well suited for this purpose and a number of effects revealing the influence of the pore walls on the dynamic properties of the confined liquid have been elucidated [5–7]. Notably, in parallel to purely topological effects on molecular propagation, also the huge surface area typical of mesoporous materials with a specific molecule-pore wall interaction generates a substantial impact on molecular diffusion [8–11].

Upon variation of the temperature in bulk liquids and in liquids completely saturating porous solids, the measured diffusivities often are reasonably well described by the Arrhenius model, i.e., with diffusivities exponentially depending on reciprocal temperature [8,12]. This model implies random molecular jumps with jump rates controlled by the activation energy of molecular propagation. When molecules, however, are confined to mesopores, the intermolecular and the molecule-pore wall interactions may vary in quantitatively different ways with changing temperature. Depending on the experimental conditions, this may lead to situations where the confined liquids may undergo phase transitions [2,8,13–16]. One of the important questions to be explored in this context concerns the quantitative analysis of the temperature dependencies of measured fluid self-diffusivities in mesopores subjected to evaporation or condensation transitions upon temperature variation. It must be mentioned that irrespective of a substantial progress in the understanding of phase transitions under mesoscopic confinement achieved over the last decades [2], their alternative exploration based on fluid transport properties is still an attractive field of research which may yield additional insight into the phenomenon [4].

Diffusion in partially filled mesoporous materials, being relevant to the topic of the present study, has been the subject of a series of studies using field gradient NMR [11,17–26]. In early studies by D'Orazio *et al.* [24,25], the measured self-diffusion coefficients of water imbibed in silica gel glasses has been observed to be strongly enhanced if the pore space is only partially filled. The measurements were performed with porous glasses with pore sizes of 47 nm and 240 nm and a high value of porosity (85%). The relaxation and also diffusion data have shown that all measurements were performed over sufficiently long time scales, so that the influence of short-scale structural heterogeneities has been averaged out. This is the condition for "fast exchange" [27] in which the propagation of the guest molecules may be characterized by a single effective self-diffusion coefficient. As one of the primary results of that work, the authors observed a remarkably strong enhancement of the self-diffusion coefficient for pore fillings less than 30%. This enhancement was ascribed to the fast exchange with the vapor phase, where the diffusivities exceeded those of the bulk by several orders of magnitude. The obtained results had been satisfactorily described in terms of a two-phase model taking into account the liquid layers adsorbed on the surface and the vapor phase occupying the remaining pore volume. In sub-

*Author to whom correspondence should be addressed. Electronic address: valiullin@uni-leipzig.de

sequent studies [28], a qualitatively different pattern of the concentration dependence of the diffusivity of water in 3.5 nm porous glass has been reported. The result was attributed to a substantially smaller influence of the Knudsen diffusivity in the gas phase due to much smaller pore sizes.

More recent work [18,22,23,29] emphasizes that the influence of diffusion acceleration by the Knudsen mechanism most decisively depends on the relative number of molecules undergoing this mechanism. This correlation appears, e.g., in the fact that in Ref. [18] it was found that water and cyclohexane molecules exhibit qualitatively dissimilar concentration dependencies of diffusivities in Vycor porous glass with 4 nm pore size. The analogous differences have been observed in VitraPore silica glass with 1 μm pore size [29]. While this correlation leading to effective diffusivities much larger than those in the liquid bulk phase [30] was well understood and employed for modeling diffusion in the void ("intercrystalline") space between nanoporous particles (zeolite crystallites) [31,32], now similar considerations emerged also for PFG NMR diffusion studies with mesoporous materials.

Diffusion studies with alkane molecules in mineral clays exhibiting a mesoporous structure were performed by Maklakov and Dvoyashkin [21,33–35]. To our knowledge, in these studies for the first time molecular diffusion in mesoporous host-guest systems has been investigated by correlating both the loading and temperature dependence. Only on the basis of this correlation and of the resulting estimate of the influence of the diffusivities in the bulk phase and in the free space within the pore systems, the previously stated anomalies in the loading dependence of the diffusivities could be rationalized. One of the remarkable results of these studies was the strong influence of the temperature on the dependence of the diffusivity on the concentration. While at sufficiently low temperatures the diffusivities monotonically increased with loading, at higher temperature the loading dependence of the diffusivities revealed pronounced minima. This was directly shown for the system tridecane-kaolinite for the temperature range 303 K–383 K [21].

The explanation of these phenomena is based on the different modes of diffusion within the system and their temperature dependence and has been checked for several values of the pore filling factor including the case of over-saturated samples with an excess liquid fraction outside the particles of the sample [35]. For a given concentration, deviations from the monoexponential form of the measured spin-echo attenuation functions (indicating that the overall diffusion behavior must be described by more than one diffusivity) have been observed in the high-temperature region. By contrast, at low temperatures monoexponential behavior was approached, with a slope (corresponding to the effective diffusivity) close to that of the bulk fluid. The deviation from monoexponential behavior observed at high temperatures was attributed to the presence of saturated vapor in the pore cavities the influence of which start to be essential at a certain temperature. It must be noted that for the overloaded samples the activation energy for diffusion was found to be almost the same as that of the bulk in the whole temperature range covered in the experiment.

Recently, in Refs. [22,23,36] detailed knowledge of the gas phase pressure (and, hence, of the gas phase concentration) as a function of the amount of guest molecules contained in the mesoporous media has been used for the prediction of the effective diffusivities. The measurements have been performed using model silica wafers containing arrays of parallel cylindrical channels with diameters between 5 and 10 nm and with Vycor random porous glass with a pore size of about 5 nm at temperatures notably below the boiling temperature of the guest fluid. The diffusivities, calculated by means of two-phase exchange model, with corresponding weighting factors obtained by explicit use of the adsorption isotherms, have been shown to quantitatively well describe the experimental data.

In the present study, we have focused on the effect of temperature on the diffusion properties of fluids in mesopores. Commonly, the PFG NMR experiments are performed using sealed samples. Thus, depending on the initial amount of the liquid in a sample, variation of temperature may lead to temperature-driven adsorption or desorption, and may alter, therefore, the phase conditions within the mesopores. In turn, this would lead to a more complex variation of the measured effective diffusivities as compared to the Arrhenius pattern. While this picture has qualitatively been observed in the experiments, so far no detailed analysis of molecular transport under the discussed conditions have been provided. Here, by exploiting the macroscopically extended mesoporous particles of Vycor porous glass, such a quantification has been possible due to the known morphology of the porous space and the precise control of the relevant external parameters during the diffusion studies.

II. EXPERIMENT

Vycor porous glass [37] (No. 7930, 96% SiO_2) was purchased from Corning Inc., Corning, NY, USA. This porous material is characterized to have a highly interconnected network of pores [38,39]. The average pore diameter specified by the manufacturer is 4 nm (96% of the pore volume is within 4 ± 0.6 nm), the porosity is 28% and the specific surface is 250 m^2/g. This material tends to adsorb organic vapors from the air. In order to remove such impurities and following the recommendations of the manufacturer, the samples were boiled in 30% H_2O_2 for several hours at 373 K. The liquid under study, *n*-pentane, was purchased from Merck (Merck, Germany) and used without further purification.

Two types of samples (Fig. 1) have been prepared which provide two distinctly different conditions for the coexistence of the intrapore fluid and the outer phase. The well-known adsorption phenomenon [40] has been used for preparing the samples. The first sample, an NMR glass tube with initially outgassed Vycor porous glass, has been kept at a vapor pressure close to the saturated vapor pressure P_s of *n*-pentane (namely at approximately 0.9 P_s) at $T=240$ K. This procedure ensures that the pore interior is completely saturated, without the formation of any excess liquid. In what follows, this sample will be referred to as the QS sample. The second sample was saturated with *n*-pentane under vacuum until the rod of Vycor porous glass was completely sunk. This sample, with excess *n*-pentane, is referred to as

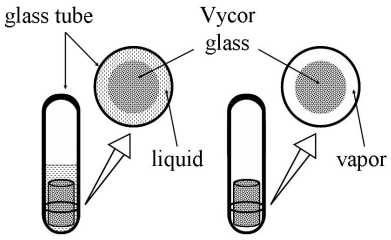

FIG. 1. Sketch of two samples used for the experiments. The first sample is oversaturated by the liquid (QE, left-hand panel), while in the second sample only the mesopores are saturated by the liquid (QS, right-hand panel).

the QE sample. The latter procedure yields total absence of any phase boundaries (meniscuses) between the intrapore and the excess liquid. In contrast to this, the QS sample is characterized by the coexistence of a capillary-condensed phase in the pores and a gas phase outside, with a liquid-gas interface in-between. In terms of pore filling factors (referring to only the mesopores), the QS sample has a value close to 1 at low temperatures, while, invariably, it is almost 1 for the other sample. The pore filling factor is defined as the ratio between the total volume of the liquid in the samples and the total pore volume of the Vycor glass.

The PFG NMR method has been employed as a well-suited, noninvasive tool in all sets of our diffusion measurements [5,6]. Diffusion experiments were performed on an NMR spectrometer operating at a 400 MHz resonance frequency for protons. It was equipped with a home-built pulsed field gradient unit producing a maximal z-gradient strength of about 35 T/m in a 7 mm o.d. NMR sample [41]. We have applied the 13-interval stimulated-echo pulse sequence with bipolar gradients (Fig. 2) [42] in order (i) to minimize the effect of internal magnetic fields originating from susceptibility differences between the fluid and porous material and (ii) to suppress undesirable eddy current effects [43,44]. Typical parameters of the pulse sequence used were $\tau=1$ ms, $\delta=400$ μs, and $\Delta=10$ ms. Signal accumulation was performed with a repetition time $5T_1$, where T_1 is the spin-lattice relaxation time.

For each temperature we have measured the NMR signal intensity following a single 90° radio-frequency pulse (free induction decay) which is proportional to the number of n-pentane molecules in the sample under study. This allowed us to determine the amount of both the liquid and gas molecules by placing the NMR sample coil around either the rod

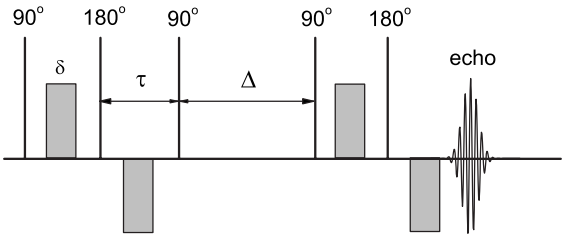

FIG. 2. The 13-interval stimulated-echo pulse sequence. The filled rectangles represent gradient pulses with length δ and variable amplitude g.

of porous glass or the free space above. The repetition time between pulses has been chosen to obey the relaxation requirements of the system under study. Thus, to measure the signal of n-pentane in the gaseous phase the repetition time varied from 5 s at the lowest temperature to 50 s at the highest temperature. The influence of the Curie effect, namely the temperature-dependent character of nuclear magnetization, has been taken into account. Details of this procedure are given in the Appendix. The precision of the temperature measurement was 0.1 K.

III. RESULTS AND DISCUSSION

A. Phase equilibria

The sample QE contains a sufficiently large amount of liquid in excess, so that even at the highest temperatures considered in our studies (380 K) the saturated vapor pressure over the fluid does not totally consume the liquid phase outside of the pore space. Therefore, over the total temperature range 240–380 K studied, the gas pressure (and hence the molecular concentration in the gas phase) is that of the saturated vapor pressure of the liquid at the given temperature. As a consequence, the pores shall remain completely filled by the liquid in all experiments.

A completely different situation is expected for the sample QS, which contains just such an amount of n-pentane that at the lowest temperature $T=234$ K the pore space is completely filled, while the outer space is only occupied by the gas phase, namely by the vapor of the guest liquid residing in the pores. Thus, in contrast to the sample QE, the sealed sample tube QS does not contain a sufficiently large amount of molecules which would simultaneously guarantee the total pore filling and the maintenance of the saturated vapor pressure in the space around the porous material.

The consequences of this situation on the actual loading of the porous material with increasing temperature are demonstrated by Fig. 3. It displays the relative number (normalized concentration) θ of guest molecules in the mesopores as a function of temperature. θ is defined as the ratio between the number of molecules accommodated by the pore space at a given temperature and their number at the lowest temperature $T=234$ K. Recall that the number of molecules is directly proportional to the free induction decay signal. The figure provides a comparison between the actually measured amount of n-pentane molecules residing in the pore space with the amount which would be accommodated at the given temperature at total pore filling. The dramatic decrease to about 37% of the initial value in the actual loading is thus shown to be by far not a simple consequence of density decrease with increasing temperature. It reflects the fact that, with increasing temperature, in an increasing part of the pore system the guest molecules are in the gaseous rather in the liquid state.

Obviously, temperature enhancement (reduction) is accompanied by the evaporation (condensation) of a part of the guest molecules within the pore system. Most remarkably, in the temperature range between $T=300$ K and $T=350$ K, our data even reflect indications of sorption hysteresis, i.e., of the history dependence of the actual loading in mesopores [40].

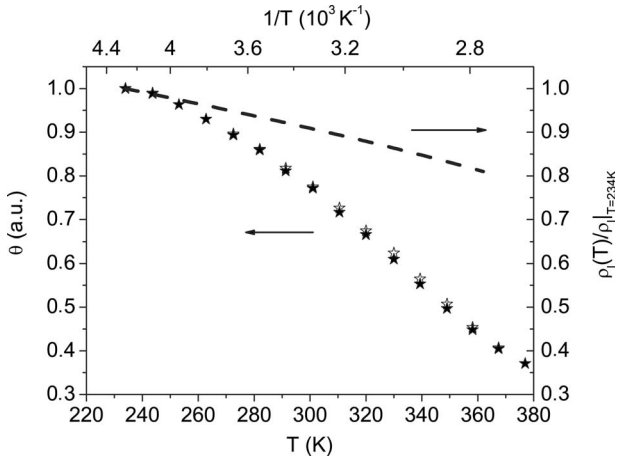

FIG. 3. Relative amount (i.e., normalized concentration) θ of *n*-pentane molecules in the mesopores of the sample QS as a function of temperature (left-hand axis). The open and filled stars refer to the heating and to the cooling branches, respectively. The variation of the normalized density of bulk *n*-pentane with changing temperature under saturation conditions is shown by the dashed line (right-hand axis, taken from Ref. [45]).

With a maximum difference of 3% for the total amount adsorbed during temperature increase (i.e., during desorption) and during temperature increase (i.e., during adsorption) at $T=330$ K, this effect is not very pronounced. This difference, however, exceeds the uncertainty of our measurements ($\pm 1\%$ in the relevant range) and is well reproducible.

By showing the temperature dependence of the vapor pressure above the porous material, Fig. 4 represents the counterpart of the just discussed situation within the pore space. The actual pressure P in the gas phase in the sample QS was calculated using the van der Waals equation

$$\left(P + a_{\text{pent}}\frac{N^2}{V^2}\right)(V - Nb_{\text{pent}}) = NRT, \tag{1}$$

with the constants a_{pent} and b_{pent} for *n*-pentane 19.26 l^2 bar/mol^2 and 0.146 l/mol, respectively. In Eq. (1), V is the known volume accessible for the gas phase and N is the mole number of molecules in the gas phase. The latter quantity was directly assessed by measuring the NMR free induction decay signal intensity in the gas phase. In addition to the measured values, Fig. 4 contains the temperature dependence of the vapor pressure resulting in the two relevant limiting cases. The dashed line simply represents the saturated vapor pressure. The full line results by application of Eq. (1) where the number of molecules in the gas phase has been determined by keeping the pore filling factor equal to 1 over the whole temperature range studied. In this estimate, the density of the liquid in the pores has varied with changing temperature as in the bulk liquid. Thus, the expansion of the liquid in pores led to the transfer of some amount of the molecules to the surrounding gas phase.

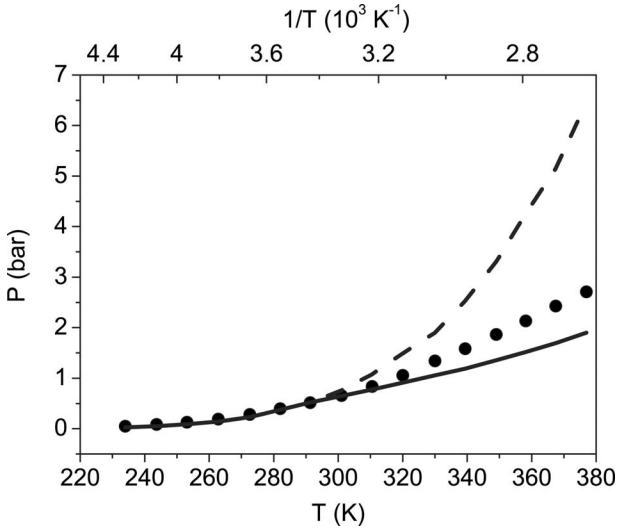

FIG. 4. The measured gas pressure (filled circles) in the empty volume of the glass tube of the sample QS as a function of temperature. The dashed line shows the saturated vapor pressure of *n*-pentane at different temperatures. The solid line represents a hypothetical pressure which would be attained if transfer of the intraporous molecules into the gas phase would be controlled exclusively by the change of the liquid density. See the text for more details.

It is worth noting that the curves shown by the dashed and solid lines may be considered to represent the limiting cases of (i) weak and (ii) strong surface tensions, respectively. Thus, in the former case (i), the liquid readily evaporates from the pores upon increasing temperature in order to provide the saturated conditions in the surrounding gas phase. This may be achieved both due to a progressive invasion of the gas phase into the pores and the cavitation of bubbles within the porous system [46–49]. In the latter case (ii), both processes are prohibited and the gas-condensed liquid interface remains intact. The actually measured temperature dependence of the vapor pressure within the sample QS is found to be between these two limiting cases. As stated above, the limited amount of guest molecules within the sample tube prohibits the simultaneous maintenance of total pore filling and vapor pressure saturation in the free space of the sample. Thus, our experimental finding reveals that the pore system is necessarily not completely filled with the guest molecules. However, the evaporation and/or condensation process is controlled not only by the gas pressure but also by the capillary forces preventing complete desorption and/or adsorption as in bulk liquids.

B. Molecular diffusion

In this section we provide the results of our PFG NMR diffusion measurements. With the experimental data shown in Figs. 3 and 4, we dispose of the key parameters controlling molecular diffusion in the pore system, namely the degree of their pore filling (Fig. 3) and the molecular concentration in the gas phase (Fig. 4). We shall demonstrate that these data allow a concise prediction and rationalization.

Figures 5(a) and 5(b) show the PFG NMR spin echo attenuation functions in the sample QS [Fig. 5(a)] and in the sample QE [Fig. 5(b)]. The difference in the nature of the samples is immediately revealed in the observed dependencies. In the saturated sample QS, the attenuations follow the simple monoexponential dependence,

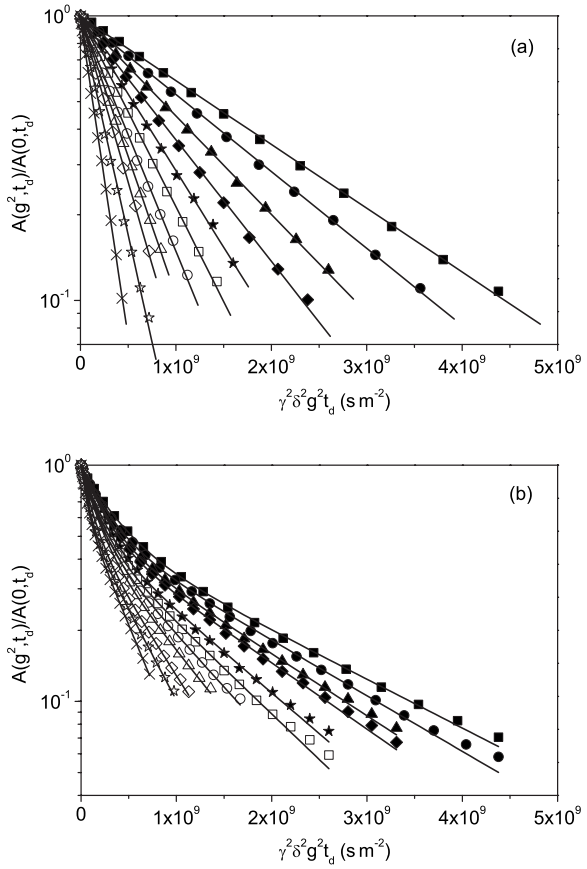

FIG. 5. PFG NMR spin-echo attenuation functions for the samples QS (no excess liquid) and QE (with excess liquid). The different symbols stand for measurements performed at different temperatures from $T=228$ K (filled squares) to $T=353$ K (crosses). The solid lines show the best fit to the experimental data using Eq. (2) (a) and the superposition of two equations of the structure of Eq. (2) with corresponding weighting fractions (b), respectively.

$$A(g^2,t_d) = A(0,t_d)\exp\{-\gamma^2 g^2 \delta^2 D_{\text{eff}} t_d\}, \tag{2}$$

as to be expected for a (quasi)homogeneous system [5,6]. The diffusivity D_{eff} appearing in Eq. (2) is that of the *n*-pentane molecules confined to the Vycor pore system, i.e., reduced by the tortuosity factor as compared to the bulk diffusivity D_0 [7]. In the oversaturated sample QE, however, a notable deviation from the monoexponential dependence is observed, which may easily be attributed to the fact that, in addition to the molecules within the pore system, there is a substantial fraction of *n*-pentane molecules also outside of the pore space, forming a bulk liquid. Since the macroscopic dimensions of these two regions (millimeters) are much larger than the diffusion paths probed (micrometers), any substantial molecular exchange between these regions during the observation time of the NMR experiments (milliseconds) is excluded. Thus, the spin-echo attenuations are given just by the superposition of two exponentials of the form of Eq. (2) with the prefactors representing the relative fractions of *n*-pentane molecules inside and outside of the Vycor pore system. Since, for the given system, the relaxation times of transverse and longitudinal nuclear magnetization (hundreds

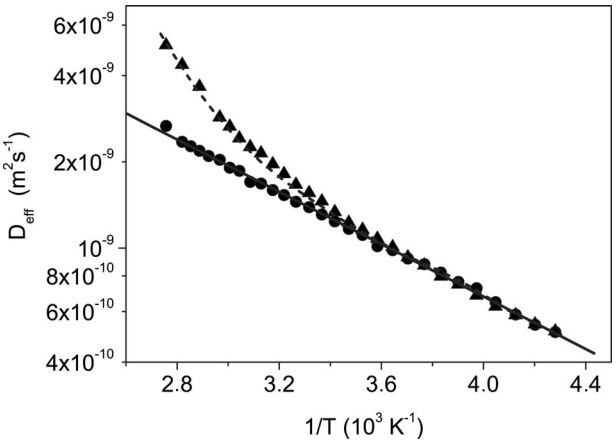

FIG. 6. Effective intrapore diffusion coefficients obtained from diffusion spin-echo attenuations in Fig. 5 for the sample QE with excess bulk liquid (filled circles) and for the sample QS without excess liquid phase (filled triangles). The solid line shows fit of Eq. (8) to the data shown by circles. The dashed line is Eq. (3) with all relevant parameters discussed in the text (no fit).

of milliseconds and seconds) are found to notably exceed the time intervals of the PFG NMR pulse sequence in Fig. 2, there is no need for a relaxation-dependent correction of these fractions. Importantly, no observation time dependence in the time interval Δ from 5 to 100 ms has been observed. The full lines in Figs. 5(a) and 5(b) represent the fits to the experimental data using Eq. (2) and biexponential functions, respectively. In the latter case, the contribution with the smaller slope and hence with the smaller effective diffusivities represents the liquid confined to the Vycor pore system with the corresponding relative fraction.

In Fig. 6, the thus obtained diffusivities D_{eff} of solely guest molecules in the Vycor porous glass are shown in the Arrhenius coordinates for both samples under study. Not unexpectedly, in the low-temperature range there is a nice agreement between these two data sets which, moreover, follow the Arrhenius dependence. Starting from about $T=300$ K, however, the effective intraporous diffusivities in sample QS notably deviate to higher values. This anomaly should obviously be attributed to the appearance of void space within the pore system with increasing temperature and can be correlated, therefore, with the information on the respective concentrations in Fig. 3.

The quantitative estimate of the diffusivity within the Vycor pore system can be based on the equilibrium data deduced in the preceding section. For this purpose, we use the two-region approach of PFG NMR diffusion measurements [27,50,51], where the effective diffusivity results as the mean value of the diffusivities in the different regions relevant for molecular propagation. In the given case we have

$$D_{\text{eff}} = p_l D_l + p_g D_g = (1-p_g)D_l + p_g D_g, \tag{3}$$

with the quantities D and p denoting the diffusivities in the different regions and their respective populations and the indices l and g referring to the liquid and the gaseous phases within the pores, respectively. It is worth noting that Eq. (3) can be obtained using the following phenomenological ap-

proach. First, we decompose a trajectory sampled by a molecule during an observation time t on sections corresponding to displacements $\vec{r}_{l,i}$ and $\vec{r}_{g,i}$ in different phases. Here, the indices i refer to the subsequent alternating displacements in different phases. Thus, for a molecule starting, e.g., at an origin located in the liquid phase, D_{eff} may be defined using the Einstein equation

$$D_{\text{eff}} = \frac{a}{t}(\vec{r}_{l,1} + \vec{r}_{g,2} + \vec{r}_{l,3} + \vec{r}_{g,4} + \cdots)^2, \tag{4}$$

where a is the dimension-dependent numerical constant. Combining all displacements in one phase and making use of the stochastic character of the self-diffusion process, Eq. (4) may be rewritten as

$$D_{\text{eff}} = \frac{a}{t}\sum_i (\vec{r}_{l,i})^2 + \frac{a}{t}\sum_j (\vec{r}_{g,j})^2. \tag{5}$$

Since operating under equilibrium conditions, detailed balance immediately leads to Eq. (3) with p_l and p_g being the fractions of time spent in the phases l and g, respectively.

To estimate the quantity p_g, the single cylindrical pore model [22] has been considered. Accordingly,

$$p_g = \frac{1-\theta}{\theta}\frac{\rho_g}{\rho_l}, \tag{6}$$

where the density ρ_g in the gas phase is, in a first approximation, given by the ideal gas law $\rho_g = P_{g,\text{ext}}/RT$ with $P_{g,\text{ext}}$ being the vapor pressure in glass tube. We further assume that the density of the adsorbed phase in Eq. (6) is the same as for n-pentane in the liquid state. The concentrations θ are those given in Fig. 3.

In order to estimate the diffusivities in the gaseous phase within the pore space, the character of the condensed phase distribution must be assessed. Earlier studies suggest different possible scenarios [26,52,53]. In [26], the PFG NMR study of n-hexane distribution within Bioran random glass with an average pore size of 40 nm at room temperatures revealed that the condensed phase at partial pore fillings forms a central kernel or an extended single capillary-condensed "droplet" with typical size of a few tens of micrometers. The pore space remaining between the liquid kernel ("droplet") and the particle boundary is characterized by multilayer adsorption on the surface. In our case, such a situation would imply two macroscopically separated extended regions, both of which would exhibit different diffusion properties, and result in a nonexponential character of the spin-echo attenuations. As shown in Fig. 5(a), this is not the case. We, thus, anticipate that under the experimental conditions of our study the combined effect of cavitation and pore blocking phenomena [46–49] leads to a quasihomogeneous distribution of cavities and capillary condensate over the scale of the PFG NMR experiments. Such a distribution could formally be referred to as a plug-model [53,54]. It has been shown recently that the activated nature of density redistribution in this case prevents the system from equilibration [4]. Presumably, at equilibrium, which is not attained under our experimental conditions, the density distribution would correspond to the kernel model of Ref. [26].

The diffusivity in the gaseous phase is controlled by collisions with the gas-liquid interface and by intermolecular collisions. Recalling the discussion of Eqs. (4) and (5), by collisions we may understand hitting-reflection events at the interface as well as events composed of adsorption-diffusion within liquid phase-desorption processes. Due to the small pore sizes and relatively low gas densities, intermolecular collisions turn out to have a negligible effect on the molecular paths in the gaseous phase in the pores. Thus, the concept of Knudsen diffusion may be applied. For cylindrical pores of diameter d the corresponding diffusivity D_K is [55,56]

$$D_K = \frac{d}{3}\sqrt{\frac{8RT}{\pi M}}, \tag{7}$$

where R is the universal gas constant and M is the molar mass. The actual value of d in Eq. (7) must be corrected by the thickness of the adsorbed layer.

For the liquid phase in the pores (the capillary-condensed phase and the multilayered molecules on the pore walls) we assumed that the diffusion coefficient follows the Arrhenius behavior,

$$D_l = D_p \exp\left\{-\frac{E_D}{RT}\right\}, \tag{8}$$

where E_D is the activation energy of molecular diffusion. The parameters $D_p = 4.5\times 10^{-8}\ \text{m}^2\ \text{s}^{-1}$ and $E_D = 8.7(\pm 0.2)$ kJ/mol have been used as obtained from the fitting to the data obtained for the sample QE in Fig. 6. Notably, the low-temperature part for D_{eff} in the sample QS has the same activation energy. The obtained activation energy is in good agreement with the literature value $E_D \approx 8.0$ kJ/mol for bulk n-pentane in the given temperature range [57,58].

Finally, the effective diffusivities for n-pentane in the sample QS may be predicted on the basis of Eq. (3) with (i) the weighting factors given by Eq. (6) with ρ_g directly related to the gas pressure in the tube as shown in Fig. 4; (ii) the respective diffusivities D_g and D_l given by Eqs. (7) and (8), respectively. The thus calculated D_{eff}, as a function of temperature, is shown in Fig. 6 by the dashed line. Thus it is found that the experimentally measured effective diffusivities are in excellent agreement with the theoretical predictions of diffusivities in the Vycor pore system resulting from the analysis of their equilibrium phase behavior presented in the preceding section.

IV. CONCLUSIONS

The present study was dedicated to the study of diffusion of a liquid (n-pentane) within the pore system of Vycor porous glass in a broad temperature range including those above the boiling point of the net liquid using the PFG NMR method. With sealed samples, commonly used in NMR studies, the impact of an overall fluid content in sample tubes on the intrapore diffusion process under isochoric conditions have been addressed. In oversaturated samples, i.e., by ensuring that over the complete temperature range under consideration the pore space has been completely filled by the liquid, molecular diffusion was found to follow an Arrhenius

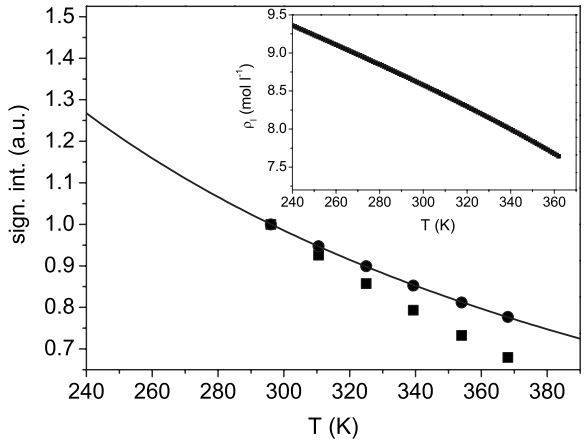

FIG. 7. Variation of the measured free induction signal intensity of bulk *n*-pentane with temperature (filled squares). The filled circles show the same signal but normalized to density variation with changing temperature. The solid line shows fit of the equation C/T to the data, where C is a fitting parameter. The inset shows the density of *n*-pentane as a function of temperature.

dependence with the activation energy for diffusion typical of the bulk liquid.

As another representative case, molecular diffusion in a sample containing an amount of guest molecules ensuring complete pore filling only at the lowest temperatures has been considered. Therefore, with increasing temperature, there is a competing process between either keeping the vapor pressure in the gas phase surrounding the porous particles saturated or keeping the intrapore liquid phase intact. At lower temperatures, up to about 300 K, undersaturation is found to be sufficiently small. This is provided by the decreasing density of the liquid in the pores and, thus, by transfer of extra molecules into the gas phase. At temperatures above 300 K, however, the latter process cannot compensate the decreased value of the vapor pressure in the gas phase as compared to the saturated one. Thus, undersaturation becomes sufficient to trigger cavitation in the sufficiently large pores of the Vycor glass. This conclusion is confirmed by both the shape of the spin-echo attenuation functions, which reveal monoexponential behavior and the absolute values of the effective diffusivity of the fluid in the pores, which is exactly reproduced by a simple microkinetic approach based on this model.

Starting from about 300 K the diffusivities obtained in these two samples start to deviate from each other. The enhancement of molecular propagation in the sample containing no excess liquid originates from the contribution of fast molecular diffusion in such cavitated regions of the porous structure. Molecular transport therein is considered to follow Knudsen diffusion, the simplest model one would imply under the given conditions. Simultaneously with the PFG NMR diffusion measurements, NMR spectroscopy as well allows a quantization of the respective phase contributions and concentrations. By means of the thus accessible equilibrium data, all features of the experimentally observed diffusion behavior could be predicted within the two-phase exchange model, without the need of any fitting parameters. In particular, the data analysis pointed out that the dramatic increase in the slope of the Arrhenius plot of the diffusivity in the sample without oversaturation results as a combined effect of the formation of internal gaseouslike filled regions and the establishment of extremely fast diffusion paths through these regions. The quantification of the structural details of these regions is the purpose of our further studies.

ACKNOWLEDGMENT

The work has been supported by the German Science Foundation (DFG) within the IRTG program "Diffusion in porous materials."

APPENDIX: CORRECTION FOR THE CURIE EFFECT

The data presented in Figs. 3 and 4 have been corrected for the Curie effect, i.e., the $1/T$ temperature dependence of nuclear magnetization. In order to take account of this effect, the free induction signal intensity in a reference sample with bulk *n*-pentane has been measured over a certain temperature range. To prevent the influence of evaporation and/or condensation on the signal intensity, the liquid height in the glass tube has always been higher as compared to the sensitive space of the NMR radio-frequency coil. The results are shown in Fig. 7. In the present setup, the apparent reduction of the NMR signal with increasing T is both due to changes of the liquid density ρ_l and equilibrium nuclear magnetization. With the known function $\rho_l(T)$, the required normalization function C/T has been obtained as shown by the solid line in Fig. 7. All data for pressure and concentration shown in Figs. 3 and 4 have been deduced from the respective NMR signal intensities by taking account of this correction factor.

[1] M. Thommes and G. H. Findenegg, Langmuir **10**, 4270 (1994).
[2] L. D. Gelb, K. E. Gubbins, R. Radhakrishnan, and M. Sliwinska-Bartkowiak, Rep. Prog. Phys. **62**, 1573 (1999).
[3] R. Valiullin and A. Khokhlov, Phys. Rev. E **73**, 051605 (2006).
[4] R. Valiullin, S. Naumov, P. Galvosas, J. Karger, H. J. Woo, F. Porcheron, and P. A. Monson, Nature (London) **443**, 965 (2006).
[5] P. T. Callaghan, A. Coy, D. MacGowan, K. J. Packer, and F. O. Zelaya, Nature (London) **351**, 467 (1991).
[6] W. S. Price, Concepts Magn. Reson. **9**, 299 (1997).
[7] P. N. Sen, Concepts Magn. Reson. Part A **23A**, 1 (2004).
[8] R. Kimmich, S. Stapf, A. I. Maklakov, V. D. Skirda, and E. V. Khozina, Magn. Reson. Imaging **14**, 793 (1996).
[9] J. P. Korb, M. Whaley-Hodges, and R. G. Bryant, Phys. Rev. E **56**, 1934 (1997).
[10] E. W. Hansen, F. Courivaud, A. Karlsson, S. Kolboe, and M.

Stocker, Microporous Mesoporous Mater. **22**, 309 (1998).
[11] E. Gedat, A. Schreiber, G. H. Findenegg, I. Shenderovich, H. H. Limbach, and G. Buntkowsky, Magn. Reson. Chem. **39**, S149 (2001).
[12] M. Holz, S. R. Heil, and A. Sacco, Phys. Chem. Chem. Phys. **2**, 4740 (2000).
[13] Y.-C. Liu, Q. Wang, and L.-H. Lu, J. Chem. Phys. **120**, 10728 (2004).
[14] D. W. Aksnes, L. Gjerdaker, L. Kimtys, and K. Forland, Phys. Chem. Chem. Phys. **5**, 2680 (2003).
[15] D. W. Aksnes, K. Forland, and M. Stocker, Microporous Mesoporous Mater. **77**, 79 (2005).
[16] S. Qiao and S. Bhatia, Microporous Mesoporous Mater. **86**, 112 (2005).
[17] I. Ardelean, C. Mattea, G. Farrher, S. Wonorahardjo, and R. Kimmich, J. Chem. Phys. **119**, 10358 (2003).
[18] I. Ardelean, G. Farrher, C. Mattea, and R. Kimmich, Magn. Reson. Imaging **23**, 285 (2005).
[19] S. R. Veith, E. Hughes, G. Vuataz, and S. E. Pratsinis, J. Colloid Interface Sci. **274**, 216 (2004).
[20] F. Courivaud, E. W. Hansen, S. Kolboe, A. Karlsson, and M. Stocker, Microporous Mesoporous Mater. **37**, 223 (2000).
[21] N. K. Dvoyashkin, V. D. Skirda, A. I. Maklakov, M. Belousova, and R. Valiullin, Appl. Magn. Reson. **2**, 83 (1991).
[22] R. Valiullin, P. Kortunov, J. Kärger, and V. Timoshenko, J. Chem. Phys. **120**, 11804 (2004).
[23] R. Valiullin, P. Kortunov, J. Kärger, and V. Timoshenko, Magn. Reson. Imaging **23**, 209 (2005).
[24] F. D'Orazio, S. Bhattacharja, W. P. Halperin, and R. Gerhardt, Phys. Rev. Lett. **63**, 43 (1989).
[25] F. D'Orazio, S. Bhattacharja, W. P. Halperin, and R. Gerhardt, Phys. Rev. B **42**, 6503 (1990).
[26] R. R. Valiullin, V. D. Skirda, S. Stapf, and R. Kimmich, Phys. Rev. E **55**, 2664 (1997).
[27] J. Kärger, H. Pfeifer, and W. Heink, Adv. Magn. Reson. **12**, 2 (1988).
[28] F. D'Orazio, S. Bhattacharja, W. P. Halperin, K. Eguchi, and T. Mizusaki, Phys. Rev. B **42**, 9810 (1990).
[29] I. Ardelean, G. Farrher, C. Mattea, and R. Kimmich, J. Chem. Phys. **120**, 9809 (2004).
[30] J. Kärger, H. Pfeifer, E. Riedel, and H. Winkler, J. Colloid Interface Sci. **44**, 187 (1973).
[31] J. Kärger and P. Volkmer, J. Chem. Soc., Faraday Trans. 1 **76**, 1562 (1980).
[32] J. Kärger and D. Ruthven, *Diffusion in Zeolites and Other Microporous Solids* (Wiley, New York, 1992).
[33] N. K. Dvoyashkin and A. I. Maklakov, Colloid J. USSR **53**, 532 (1991).
[34] A. I. Maklakov, N. K. Dvoyashkin, and E. V. Khozina, Colloid J. **55**, 79 (1993).
[35] A. I. Maklakov, N. K. Dvoyashkin, E. V. Khozina, and V. D. Skirda, Colloid J. **57**, 50 (1995).
[36] J. Kärger, R. Valiullin, and S. Vasenkov, New J. Phys. **7**, 15 (2005).
[37] T. H. Elmer, *Engineered Materials Handbook* (ASM International, Materials Park, OH, 1992), Vol. 4, pp. 427–432.
[38] P. Levitz, G. Ehret, S. K. Sinha, and J. M. Drake, J. Chem. Phys. **95**, 6151 (1991).
[39] E. S. Kikkinides, M. E. Kainourgiakis, K. L. Stefanopoulos, A. C. Mitropoulos, A. K. Stubos, and N. K. Kanellopoulos, J. Chem. Phys. **112**, 9881 (2000).
[40] C. G. V. Burgess, D. H. Everett, and S. Nuttall, Pure Appl. Chem. **61**, 1845 (1989).
[41] P. Galvosas, F. Stallmach, G. Seiffert, J. Kärger, U. Kaess, and G. Majer, J. Magn. Reson. **151**, 260 (2001).
[42] R. M. Cotts, M. J. R. Hoch, T. Sun, and J. T. Markert, J. Magn. Reson. (1969-1992) **83**, 252 (1989).
[43] D. H. Wu, A. D. Chen, and C. S. Johnson, J. Magn. Reson., Ser. A **115**, 260 (1995).
[44] G. H. Sorland and D. Aksnes, Magn. Reson. Chem. **40**, S139 (2002).
[45] National Institute of Standards and Technology, www.nist.gov/. The density of *n*-pentane at saturated conditions.
[46] E. S. Kikkinides, M. E. Kainourgiakis, and A. K. Stubos, Langmuir **19**, 3338 (2003).
[47] H. J. Woo, F. Porcheron, and P. A. Monson, Langmuir **20**, 4743 (2004).
[48] L. Sarkisov and P. A. Monson, Langmuir **17**, 7600 (2001).
[49] P. Ravikovitch and A. Neimark, Langmuir **18**, 9830 (2002).
[50] J. Kärger, Adv. Colloid Interface Sci. **23**, 129 (1985).
[51] W. S. Price, in *Diffusion Fundamentals I*, edited by J. Kärger, P. Heitjans, and F. Grinberg (www.diffusion-fundamentals.org) (Leipziger Universitatsverlag, Leipzig, 2005), pp. 490–508.
[52] S. G. Allen, P. C. L. Stephenson, and J. H. Strange, J. Chem. Phys. **106**, 7802 (1997).
[53] W. Troyer, R. Holly, H. Peemoeller, and M. Pintar, Solid State Nucl. Magn. Reson. **28**, 238 (2005).
[54] A. J. Liu, D. J. Durian, E. Herbolzheimer, and S. A. Safran, Phys. Rev. Lett. **65**, 1897 (1990).
[55] W. G. Pollard and R. D. Present, Phys. Rev. **73**, 762 (1948).
[56] P. Levitz, J. Phys. Chem. **97**, 3813 (1993).
[57] E. Fishman, J. Phys. Chem. **59**, 469 (1955).
[58] D. C. Douglass and D. W. McCall, J. Phys. Chem. **62**, 1102 (1958).